Research Article

MOLECULAR PAIN

Molecular Pain
Volume 15: 1–14

DOI: 10.1177/1744806919849802
journals.sagepub.com/home/mpx
SAGE

A gain-of-function sodium channel β2-subunit mutation in painful diabetic neuropathy

Matthew Alsaloum[1, 2, 3], Mark Estacion[1, 2], Rowida Almomani[4, 5], Monique M Gerrits[4, 6], Gidon J Bönhof[7], Dan Ziegler[7, 8, 9], Rayaz Malik[10, 11], Maryam Ferdousi[11], Giuseppe Lauria[12, 13], Ingemar SJ Merkies[6, 14], Catharina G Faber[6], Sulayman Dib-Hajj[1, 2] and Stephen G Waxman[1, 2]; on behalf of the Propane Study Group*

Abstract

Diabetes mellitus is a global challenge with many diverse health sequelae, of which diabetic peripheral neuropathy is one of the most common. A substantial number of patients with diabetic peripheral neuropathy develop chronic pain, but the genetic and epigenetic factors that predispose diabetic peripheral neuropathy patients to develop neuropathic pain are poorly understood. Recent targeted genetic studies have identified mutations in α-subunits of voltage-gated sodium channels (Na_vs) in patients with painful diabetic peripheral neuropathy. Mutations in proteins that regulate trafficking or functional properties of Na_vs could expand the spectrum of patients with Na_v-related peripheral neuropathies. The auxiliary sodium channel β-subunits (β1–4) have been reported to increase current density, alter inactivation kinetics, and modulate subcellular localization of Na_v. Mutations in β-subunits have been associated with several diseases, including epilepsy, cancer, and diseases of the cardiac conducting system. However, mutations in β-subunits have never been shown previously to contribute to neuropathic pain. We report here a patient with painful diabetic peripheral neuropathy and negative genetic screening for mutations in *SCN9A*, *SCN10A*, and *SCN11A*—genes encoding sodium channel α-subunit that have been previously linked to the development of neuropathic pain. Genetic analysis revealed an aspartic acid to asparagine mutation, D109N, in the β2-subunit. Functional analysis using current-clamp revealed that the β2-D109N rendered dorsal root ganglion neurons hyperexcitable, especially in response to repetitive stimulation. Underlying the hyperexcitability induced by the β2-subunit mutation, as evidenced by voltage-clamp analysis, we found a depolarizing shift in the voltage dependence of Na_v1.7 fast inactivation and reduced use-dependent inhibition of the Na_v1.7 channel.

[1]Department of Neurology, Yale University School of Medicine, New Haven, CT, USA
[2]Center for Neuroscience and Regeneration Research, Veterans Affairs Medical Center, West Haven, CT, USA
[3]Interdepartmental Neuroscience Program, Yale University School of Medicine, New Haven, CT, USA
[4]Department of Clinical Genomics, University Medical Center Maastricht, Maastricht, the Netherlands
[5]Department of Medical Laboratory Sciences, Jordan University of Science and Technology, Irbid, Jordan
[6]Department of Neurology, University Medical Centre Maastricht, Maastricht, the Netherlands
[7]Institute for Clinical Diabetology, German Diabetes Center, Leibniz Center for Diabetes Research at Heinrich Heine University, Düsseldorf, Germany
[18]German Center for Diabetes Research, München-Neuherberg, Germany
[9]Division of Endocrinology and Diabetology, Medical Faculty, Heinrich Heine University, Düsseldorf, Germany
[10]Weill Cornell Medicine-Qatar, Doha, Qatar
[11]Division of Diabetes, Endocrinology and Gastroenterology, Institute of Human Development, University of Manchester, Manchester, UK
[12]Neuroalgology Unit, IRCCS Foundation "Carlo Besta" Neurological Institute, Milan, Italy
[13]Department of Biomedical and Clinical Sciences "Luigi Sacco," University of Milan, Milan, Italy
[14]Department of Neurology, St. Elisabeth Hospital, Willemstad, Curaçao

*Details of the members of the Propane Study Group are given in Acknowledgments.

Corresponding Author:
Stephen G Waxman, Neuroscience and Regeneration Research Center, VA Connecticut Healthcare System, 950 Campbell Avenue, Bldg. 34, West Haven, CT 06516, USA.
Email: stephen.waxman@yale.edu

Keywords
Diabetic neuropathy, voltage-gated sodium channels, sodium channel beta-subunits, neuropathic pain

Date Received: 6 March 2019; revised: 3 April 2019; accepted: 8 April 2019

Introduction

Diabetes mellitus (DM) is one of the world's leading causes of morbidity and mortality, affecting over 425 million persons globally and costing the health-care system US$727 billion annually.[1] The health sequelae of DM are vast and encompass microvascular (retinopathy, neuropathy, and nephropathy) and macrovascular (coronary artery disease, peripheral vascular disease, and stroke) complications. Of these complications, diabetic peripheral neuropathy (DPN) is one of the most common, with a disease prevalence upward of 50% in patients with long-standing diabetes.[2]

DPN can be classified as autonomic or somatic, with many variants therein, of which distal symmetric polyneuropathy (DSP) is the most common.[3] DSP typically presents with a "stocking glove" distribution of sensory loss due to large-fiber involvement, although painful burning, prickling, and stabbing sensations are also often present secondary to small-fiber involvement. While the disease mechanisms underlying DM are becoming better understood,[4] the pathophysiology of DPN is still poorly characterized. Current theories center on the role of hyperglycemia in the development of neuropathy, as hyperglycemia results in a variety of cellular defects, including enhanced mitochondrial production of reactive oxygen species[5] and defects in the Na^+/K^+ pump.[6] However, given the vastly different symptomatology between painful and painless DPN, as well as the nonconcomitance between the two presentations, it is currently unknown whether painful and painless DPN represent different disease states and what factors might predispose a person with DM to develop one over the other. Consequently, we set out to identify genes that might predispose a patient to developing painful DPN.

Previous genetic studies have implicated voltage-gated sodium channels (Na_vs) in neuropathic pain syndromes associated with peripheral neuropathies.[7] Classically, gain-of-function mutations in *SCN9A*, the gene that encodes the $Na_v1.7$ sodium channel isoform, are known to cause inherited erythromelalgia (IEM),[8–12] paroxysmal extreme pain disorder (PEPD),[13–15] and other painful pain disorders including small-fiber neuropathy (SFN),[16] whereas loss-of-function mutations in this gene result in congenital insensitivity to pain.[17–19] However, other sodium channel isoforms have more recently been implicated in neuropathic pain states.[20–26] $Na_v1.6$ knockdown ameliorates mechanical allodynia after spared nerve injury,[21] and a gain-of-function $Na_v1.6$ mutation has been linked to trigeminal neuralgia.[20] Gain-of-function mutations in $Na_v1.8$ were reported in three patients with painful peripheral neuropathies.[22] Further evidence has since followed linking $Na_v1.8$ mutations to SFN.[24,27] Like $Na_v1.7$ and -1.8, mutations in $Na_v1.9$ have been reported in patients with painful peripheral neuropathies.[23,25,28] Although the contribution of these Na_vs to painful neuropathies has been thoroughly investigated, no human data to date have shown a role of the β-subunits.

The sodium channel β-subunit family consists of four genes, *SCN1B-SCN4B*, encoding four distinct proteins, β1–4, and two splice variants, β1A and β1B.[29,30] Voltage-gated sodium channels are heterotrimeric complexes, composed of one large pore-forming α-subunit and two small nonpore forming β-subunits ($\beta1/\beta3$ and $\beta2/\beta4$).[31] The β-subunits belong to the superfamily of cell adhesion molecules,[32,33] play roles in the trafficking of Na_vs[34] and modulation of Na_v function,[35] and mutations in their genes have been associated with a number of diseases, including epilepsy, cancer, and diseases of the cardiac conducting system.[29] Here, we present the first known case of a β-subunit contributing to the development of a painful phenotype in humans.

Materials and methods

Study population

For this study, 230 participants of the Probing the Role of Sodium Channels in Painful Neuropathies (PROPANE) study with painful and 317 participants with painless DPN were recruited at the University of Manchester (United Kingdom) and the German Diabetes Center (Düsseldorf, Germany) between June 2014 and September 2016. Local Medical Ethical Committees of both center approved this study. Written informed consent was obtained prior to participation in this study. The following records were collected: (1) demographic data, age of onset of complaints, duration of symptoms, altered pain sensation, medical history and family history, and prior and current neuropathic pain medication; (2) neurological examination

(muscle strength, pinprick and temperature sensation, vibration and position sense, and tendon reflexes); (3) nerve conduction studies (motor nerve conduction velocity, compound muscle action potential amplitude, distal latency: peroneal and/or tibial nerve, sensory nerve conduction velocity, and sensory nerve action potential: ulnar, median, and sural nerve); and (4) multiple questionnaires, including the 11-point Numerical Rating Scale (NRS) and Visual Analogue Scale to assess pain intensity (PI)[36] and the Neuropathic Pain Scale to evaluate 10 qualities of neuropathic pain.[37] As previously described,[38] inclusion criteria for the PROPANE study were age $\geq$18 years, type 1 or type 2 diabetes according to criteria of the American Diabetes Association, and a diagnosis of sensory, sensorimotor, and/or small-fiber DPN as possible, probable, or confirmed according to the Toronto Consensus criteria.[39] Exclusion criteria were other causes of neuropathy (hypothyroidism, renal failure, vitamin B12 deficiency, monoclonal gammopathy, alcohol abuse (>5 U/day), malignancies, drugs known to cause neuropathy) and concomitant diseases that might interfere with the participant's ability to fill in questionnaires. Painful neuropathy was diagnosed in patients with neuropathic pain[40] for more than 1 year and PI-NRS $\geq$ 4 despite analgesic treatment; painless neuropathy was diagnosed in patients with PI-NRS $\leq$3 and no need for treatment.

DNA isolation from peripheral blood

A peripheral blood sample was taken from all patients, and genomic DNA was extracted from peripheral blood by using QIAamp DNA Blood Maxi Kit/Puregene® Blood Core Kit (Qiagen, Hilden, Germany) or NucleoSpin ®8 Blood Isolation kit (Macherey-Nagel, Düren, Germany). Quality and concentration of the DNA were determined by NanoDrop (Thermo Scientific, Wilmington, DE, USA) and Qubit® 2.0 Fluorometer using the Qubit® dsDNA BR assay kit (Life technologies, Bleiswijk, The Netherlands). Isolated DNA was stored with a unique numeric code in the central DNA bank at Maastricht University Medical Centre and IRCCS Foundation "Carlo Besta" Neurological Institute.

Single-molecule molecular inversion probe-next-generation sequencing

Coding exons and exon-flanking intron sequences (±20bp) of *SCN1B-4B*, *SCN3A, SCN7A-11A* were sequenced by single-molecule molecular inversion probe-next-generation sequencing (smMIP-NGS). Three-hundred-twenty-four smMIPs were designed using a modified version of MIPgen software (http://shendurelab.github.io/MIPGEN/). The gap fill length between the extension and ligation arm (region of interest) of the smMIPs was fixed to 220–230nt. Probes were synthesized by Integrated DNA Technologies (IDT, Iowa, IA, USA).

Targeted capture with smMIPs was performed according to standard protocols.[41] In brief, after hybridization, gap filling and ligation circularized DNA molecules were used as template in a polymerase chain reaction (PCR) with universal primers complementary to the linker sequence. Sample-specific barcode sequences and Illumina adaptors were introduced during the PCR amplification step. Next, samples were pooled and purified using Ampure XP beads according to manufacturer's instructions. Pooled samples were sequenced using an Illumina NextSeq500 system, with 2×150-bp paired-end reads (Illumina, Inc., San Diego, CA, USA). Sequenced data were analyzed using an in-house smMIP-targeted NGS data analysis pipeline. Variants were included for analysis with >40× coverage and an alternative variant call of at least 20%.

To identify sequence variations in *SCN1B-4B*, *SCN3A, SCN7A-11A,* patients' coding and immediate flanking regions of these genes were compared with reference sequence GRCh37. Genetic variations detected were annotated according to the guidelines of the Human Genome Variation Society (http://www.hgvs.org/mutnomen/). Variants with a possible pathogenic effect were classified using Alamut Mutation-Interpretation Software (Interactive-Biosoftware, Rouen, France). Classification of variants was based on the practice guidelines of the Association for Clinical Genetic Science.[42] Variants of interest were confirmed by Sanger sequencing. Here, we report the smMIP-NGS results for *SCN2B*.

Molecular modeling

Protein data bank (PDB) structure 5FEB (Crystal structure of the Voltage-gated Sodium Channel β2-subunit extracellular domain) from Das et al.[43] was opened and edited in PyMol (Schrödinger, LLC).

Isolation and transfection of DRG neurons

All animal studies and procedures followed a protocol that was approved by the Veterans Administration Connecticut Healthcare System Institutional Animal Care and Use Committee. Dorsal root ganglia (DRGs) from 0 to 5 day postnatal Sprague-Dawley rats were harvested and dissociated as described previously with minor differences.[44] In brief, rat pup (P0-5) DRGs were dissociated with a 20-min incubation in 1.5 mg/mL collagenase A (Roche, Indianapolis, IN, USA) and 0.6 mM EDTA, followed by a 20-min incubation in 1.5 mg/mL collagenase D (Roche), 0.6 mM EDTA and 30 U/mL papain (Worthington Biochemical, Lakewood, NJ,

USA). DRGs were then centrifuged and triturated in 0.5 mL of DRG media containing 1.5 mg/mL bovine serum albumin (low endotoxin) and 1.5 mg/mL trypsin inhibitor (Sigma, St. Louis, MO, USA). After trituration, neurons were transfected with either human-β2-D109N or human-β2-wild type (WT) cDNA containing internal ribosome entry site (IRES)-GFP using a Nucleofector IIS (Lonza, Basel, Switzerland) and Amaxa Basic Neuron SCN Nucleofector Kit (VSPI-1003).

Transfection of HEK293 cells

Human embryonic kidney 293 (HEK293) cells stably expressing wild-type $Na_v1.7$ were transfected with either human-β2-D109N or human-β2-WT cDNA containing IRES-GFP using a LipoJet transfection kit (SignaGen Laboratories, Rockville, MD, USA). Stable cell lines originated within our laboratory and were produced using G418 (Geneticin) for cells expressing both the $Na_v1.7$ channel and the antibiotic-resistance gene on the same plasmid.

Macroscopic current recordings

Macroscopic currents were recorded from DRG neurons in both current-clamp and voltage-clamp mode and HEK293 cells in voltage-clamp mode using an EPC-10 amplifier and the PatchMaster program (HEKA Elektronik, Holliston, MA, USA) at 25°C. Patch pipettes were pulled from borosilicate glass (1.65/1.1, outside diameter/inside diameter; World Precision Instruments) using a Sutter Instruments P-97 puller and had a resistance of 0.8–1.5 MΩ.

For current-clamp recordings, the extracellular solution contained the following (in mM): 140 NaCl, 3 KCl, 2 $MgCl_2$, 2 $CaCl_2$, 10 HEPES, and 15 dextrose titrated with NaOH to a pH of 7.3. Patch microelectrodes were filled with intracellular solution containing the following (in mM): 140 KCl, 3 Mg-ATP, 0.5 EGTA, 5 HEPES, and 30 dextrose titrated with NaOH to a pH of 7.3. On the day of recordings, the extracellular and intracellular solutions were brought to osmolarities of 320 and 310mOsm, respectively, with dextrose. Whole-cell configuration was obtained in voltage-clamp mode before transitioning to current-clamp mode. Fluorescent small DRG neurons (<30 μm in diameter) with stable (<10% variation) resting membrane potentials (RMPs) more hyperpolarized than −40 mV were included in analysis. Cells with an input resistance lower than 100 MΩ were excluded from analysis. Input resistance was determined by the slope of a linear fit to hyperpolarizing responses to current steps from −5pA to −40pA in −5pA increments.

Rheobase was defined as the first current injection step that resulted in action potential firing without failure and was determined by a series of depolarizing current injections (200 ms) that increased incrementally by 5pA. Action potentials were defined as rapid increases in membrane potential to >40 mV with a total amplitude >80 mV. Action potential frequency was determined by quantifying the number of action potentials that a neuron fired after a 500-ms current injection. Action potential amplitudes, upstroke slope, and maximum rising slope were calculated in the FitMaster program (HEKA Elektronik).

When recording from DRG neurons, voltage-clamp extracellular solution contained (in mM): 70 NaCl, 70 Choline-Cl, 20 TEA-Cl, 3 KCl, 1 $CaCl_2$, 1 $MgCl_2$, 0.1 $CdCl_2$, 5 CsCl, 1 4-AP, and 10 HEPES (±300 nM tetrodotoxin (TTX)). When recording from HEK293 cells, voltage-clamp extracellular solution contained (in mM): 140 NaCl, 3 KCl, 1 $CaCl_2$, 1 $MgCl_2$, and 10 HEPES. We used a lower NaCl concentration in the bath solution for recording sodium current in DRG neurons to reduce the peak current amplitude and reduce the voltage-clamp errors due to the very large currents (>20 nA) that are recorded in the physiological sodium concentration of 140 mM. Patch microelectrodes were filled with intracellular solution containing the following (in mM): 140 CsF, 10 NaCl, 1.1 EGTA, and 10 HEPES. Both solutions were titrated to a pH of 7.3 with NaOH and brought to final osmolarity (320 mOsm for extracellular solution and 310 mOsm for intracellular solution) with dextrose on the day of recordings. Series resistance prediction and compensation (70%–90%) were applied to reduce the voltage errors. The recorded currents were digitized at a rate of 50 kHz after passing through a low-pass Bessel filter setting of 10 kHz. After achieving whole-cell configuration, a 5-min equilibration period was allowed before starting the recording. DRG neurons were held at −100 mV to prevent the inactivation of $Na_v1.9$.

Fluorescent DRG neurons under 30 μm in diameter were recorded from in the whole-cell configuration. Neurons with a peak voltage error greater than 4 mV or leak greater than 200 pA or 10% of the peak current were excluded.

Use-dependent inhibition at 20 Hz stimulation was determined by holding neurons at −80 mV for 2 ms, followed by a 10 ms step to −20 mv and measuring the charge transfer through the cell. Use-dependence curves were generated by plotting the following

$$I_{normalized} = \frac{I_{xsweep}}{I_{1stsweep}}$$

To measure sodium channel activation, DRG neurons were pulsed to a range of potentials between −120 mV and +40 mV, in 5 mV increments, for 100 ms after being held at a holding potential of −100 mV. Peak

inward currents were transformed to conductance using the equation

$$G = \frac{I}{(V_m - E_{Na})}$$

The conductance at each voltage was normalized to the maximum conductance and fit with the following Boltzmann equation to derive the activation curve

$$G = \frac{G_{min} + (G_{max} - G_{min})}{(1 + e^{(V_m - V_{0.5})/K})}$$

Peak current density was calculated as the peak current during the activation pulse normalized to the cellular capacitance.

To assess steady-state fast inactivation, DRG neurons were prepulsed to a range of voltages between −140 mV and 0 mV in 10 mV steps for 500 ms from a holding potential of −100 mV and then pulsed to a potential of −10 mV. Peak inward current was normalized to the maximum peak inward current and fit with the following Boltzmann equation to derive the inactivation curve

$$I = \frac{(I_{min} + 1)}{(1 + e^{(V_m - V_{0.5})/K})}$$

To calculate steady-state sodium channel conductance, the derived conductance–voltage curves were modulated by the sodium channel availability curves at each voltage step. Prior to modulation, each curve was interpolated to 250 points using a cubic spline interpolation method, allowing for comparison of sodium channel conductance at more voltages than initially sampled. Quality of interpolation was assessed visually.

Data analysis. Data were analyzed using FitMaster (HEKA Elektronik), Microsoft Excel, and Igor Pro 8 (WaveMetrics, Lake Oswego, OR, USA). Data are presented as means ± standard error. Student's *t* test was used to analyze all continuous data, except for use-dependence plots, for which analysis of variance (ANOVA) with repeated measures was used. All Student's *t* tests are two-tailed unless otherwise noted. Categorical data were analyzed via chi-square test.

Results

Identification of a novel variant in the coding region of the SCN2B gene

In our cohort of 230 painful and 317 painless DPN patients, smMIP-NGS of *SCN2B* revealed two heterozygous potentially pathogenic variants that were specific for the pain phenotype: c.319A>C (K107Q) and c.325G>A (D109N). Variant D109N was identified in the coding region of the *SCN2B* gene in a 61-year-old male with painful DPN, diagnosed at 42 years old with type 2 diabetes. It was not found in 317 patients with painless DPN. The D109N variant is rare in the reported exome and genome data, with an allele frequency of two in 282878 in heterozygosity and none in homozygosity.[45] As both variants K107Q and D109N were found in patients with painful diabetic neuropathy localize to similar regions of the β2-subunit, both variants merit analysis and we began by characterizing the D109N variant.

The patient has complained of numbness, burning, and "pins and needles" paresthesia in his extremities since 55 years of age (Table 1). Diagnostic testing showed reduced motor and sensory nerve conduction in his median, ulnar, common peroneal, and sural nerves. Sensory nerve action potentials were also decreased in amplitude, and the patient's DPN was graded a score of 9 and 7 on the Neuropathy Symptom Score and Neuropathy Disability Score Scales, respectively.

Variant D109N substitutes a residue on the outer surface of the β2-subunit, near the face of the cysteine responsible for the disulfide linkage to the α-subunit, potentially interacting with and altering the link between the β2 and α-subunits (Figure 1).[43]

Human β2 D109N confers hyperexcitability on DRG neurons

To test whether the identified D109N variant contributes to enhanced peripheral nerve excitation, DRG neurons were isolated from rat pups and transfected with either wild-type human β2 or the β2 D109N variant. Excitability of DRG neurons was analyzed using current-clamp recordings with sample representative traces as shown in Figure 2(a). The total action potential amplitude (Figure 2(b)) was unchanged between neurons expressing the wild-type β2-subunit and the D109N variant (113.28 ± 2.48 mV and 112.58 ± 2.85 mV, respectively, $p = 0.85$). Consequently, we also examined the maximum rising slope (Figure 2(c)), which corresponds to a time point roughly halfway through the upstroke of the action potential and found no significant difference between wild-type (97.06 ± 10.21) and mutant DRG neurons (84.71 ± 10.22, $p = 0.39$). We also examined the slope of the action potential between the threshold potential and the V_{max} to achieve a more holistic view of the entire action potential rising phase. The initiation of the action potential rising phase was determined as the initial time point where the first derivative of membrane potential with respect to time exceeded 20 mv/ms, as has been previously reported by Naundorf et al.[46] Here, we

Table 1. Clinical characteristics of a patient with identified DPN and β2 D109N mutation.

Demographic and clinical data		
Age (years)	61	
Sex	Male	
BMI (kg/m^2)	34.1	
Smoking (pack years)	40	
HbA1c[a] (%)	6.0	
HbA1c (mmol/mol)	42	
Diabetes mellitus	Type 2	
Diabetes duration (years)	19	
DPN duration (years)	8	
Neuropathic pain medication	Pregabalin 300 mg daily	
Neurological tests	Result	Evaluation[b]
Peroneal MNCV (m/s)	33	Abnormal
Median SNCV (m/s)	32	Abnormal
Ulnar SNCV (m/s)	33	Abnormal
Sural SNCV (m/s)	29	Abnormal
Median SNAP (μV)	5.3	Normal
Ulnar SNAP (μV)	6.5	Normal
Sural SNAP (μV)	4.3	Normal
VPT metacarpal (μm)	1.7	Abnormal
VPT malleolar (μm)	4.9	Abnormal
CDT hand (°C)	30.1	Normal
WPT hand (°C)	33.9	Normal
CDT foot (°C)	19.8	Normal
WDT foot (°C)	46.7	Abnormal
NSS (points)	9	Abnormal
NDS (points)	7	Abnormal
24 h average NRS pain score (points)	5 (7[c])	Abnormal

[a]HbA1c is a measure of glycated hemoglobin and the most commonly used method of evaluating glycemic control in patients with diabetes. Per the American Diabetes Association, one criterion sufficient for diagnosis of diabetes mellitus is HbA1c $\geq$ 6.5%, although patients are still considered to have diabetes if HbA1c falls <6.5% with medical treatment.
[b]Evaluation based on 5th/95th percentiles of the individual reference range; 2.5th/97.5th percentiles were used for NCVs and SNAPs.
[c]From medical history prior to analgesic treatment.
Note: BMI: body mass index; DPN: diabetic polyneuropathy; MNCV: motor nerve conduction velocity; SNCV: sensory nerve conduction velocity; SNAP: sensory nerve action potential; VPT: vibration perception threshold; CDT: cold detection threshold; WDT: warmth detection threshold; NSS: Neuropathy Symptom Score; NDS: Neuropathy Disability Score; NRS: Numerical Rating Scale; HbA1c: hemoglobin A1c; WPT: warm perception threshold.

again did not see a significant difference between DRG neurons expressing the wild-type β2-subunit (50.46 $\pm$ 4.93 mv/ms) and the D109N variant (47.57 $\pm$ 4.62, $p = 0.67$).

DRG neurons expressing the D109N variant β2-subunit also exhibited a similar RMP as DRG neurons with the wild-type β2-subunit (Figure 2(d)); neurons expressing the D109N variant had an average membrane potential of -53.7 ± 1.7 mV ($n = 21$), which was comparable to the -56.8 ± 1.8 mV ($n = 21$) resting membrane voltage of DRG neurons expressing the wild-type β2-subunit. We also quantified the excitability of DRG neurons expressing either β2-subunit via determination of the current injection necessary to elicit an action potential (Figure 2(e)). Rheobase was, similarly, unchanged by the presence of the D109N variant (213.57 $\pm$ 45.29 pA in D109N-expressing neurons vs. 278.23 $\pm$ 60.40 pA in wild-type neurons, $p = 0.39$).

DRG neurons expressing the D109N mutation, however, showed significantly increased action potential firing at larger current stimuli (300–500 pA) compared to neurons expressing the wild-type β2-subunit (Figure 3 (a), (c), and (d)). However, firing was comparable at lower current injections, and the percentage of multiply spiking neurons was not significantly different between wild-type and mutant neurons (Figure 3(b)). Taken together, these results indicate that hyperexcitability in neurons expressing the β2 D109N mutation is primarily due to increased repetitive firing, rather than a decreased threshold to first spiking.

The β2 D109N mutation reduces use-dependent charge transfer inhibition to allow for repetitive firing

Use-dependent inhibition of sodium channels has been previously shown to reduce the sustained repetitive firing in neurons.[47] To assess whether the β2 mutation results in reduced use-dependent inhibition, DRG neurons were voltage-clamped at a hyperpolarizing potential and depolarized at 20 Hz frequency; charge transfer was measured at each depolarization and normalized to the total current passed at the first stimulus. DRG neurons expressing the mutant β2-subunit exhibited significantly reduced use-dependent inhibition compared to wild-type neurons (Figure 4(a)). Neurons expressing the β2 D109N variant allowed 67.9% of total charge transfer after 1.5 s of 20 Hz stimulation, which was significantly more than the 59.1% allowed by neurons expressing the wild-type β2-subunit (significant by Bonferroni and Tukey ANOVA with repeated measures).

The mutant β2-subunit does not induce DRG neuron hyperexcitability through modulation of TTX-resistant sodium channels

Sodium channel β-subunits interact with all sodium channels α-subunits. To determine, within intact neurons, which sodium channels are modulated by the mutant β2-subunit, we conducted the same use-dependence protocol as illustrated above and measured the charge transfer before and after application of 300 nM TTX. Post-TTX application, there was no significant difference in the use-dependent inhibition of the TTX-resistant current in neurons expressing the β2

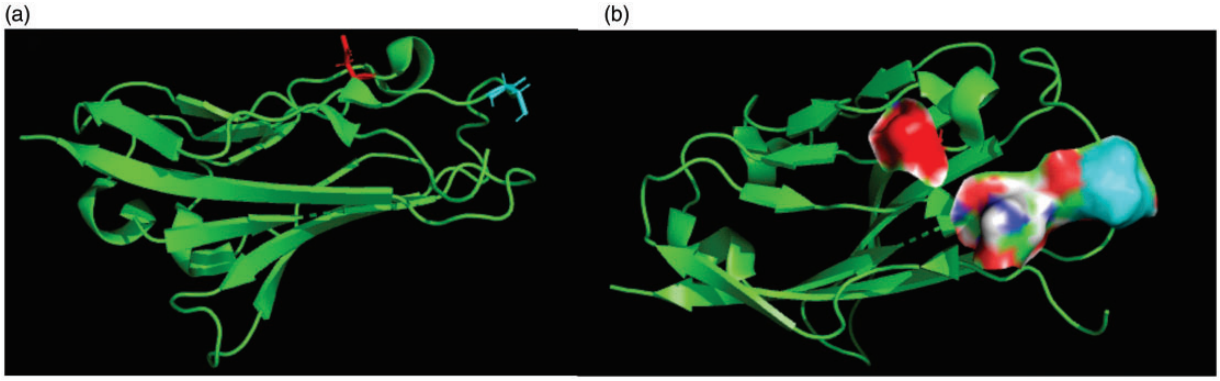

Figure 1. Structure of the β2-subunit extracellular domain illustrates the location of the D109N mutation with respect to ^{55}Cys. (a) PyMol model of the human β2-subunit with the D109 residue (red) shown near the C55 residue (cyan) responsible for disulfide bridge formation to the $Na_v1.2$ channel. (b) Surface maps illustrate a common surface between the D109 residue (red) and the C55 residue (cyan).

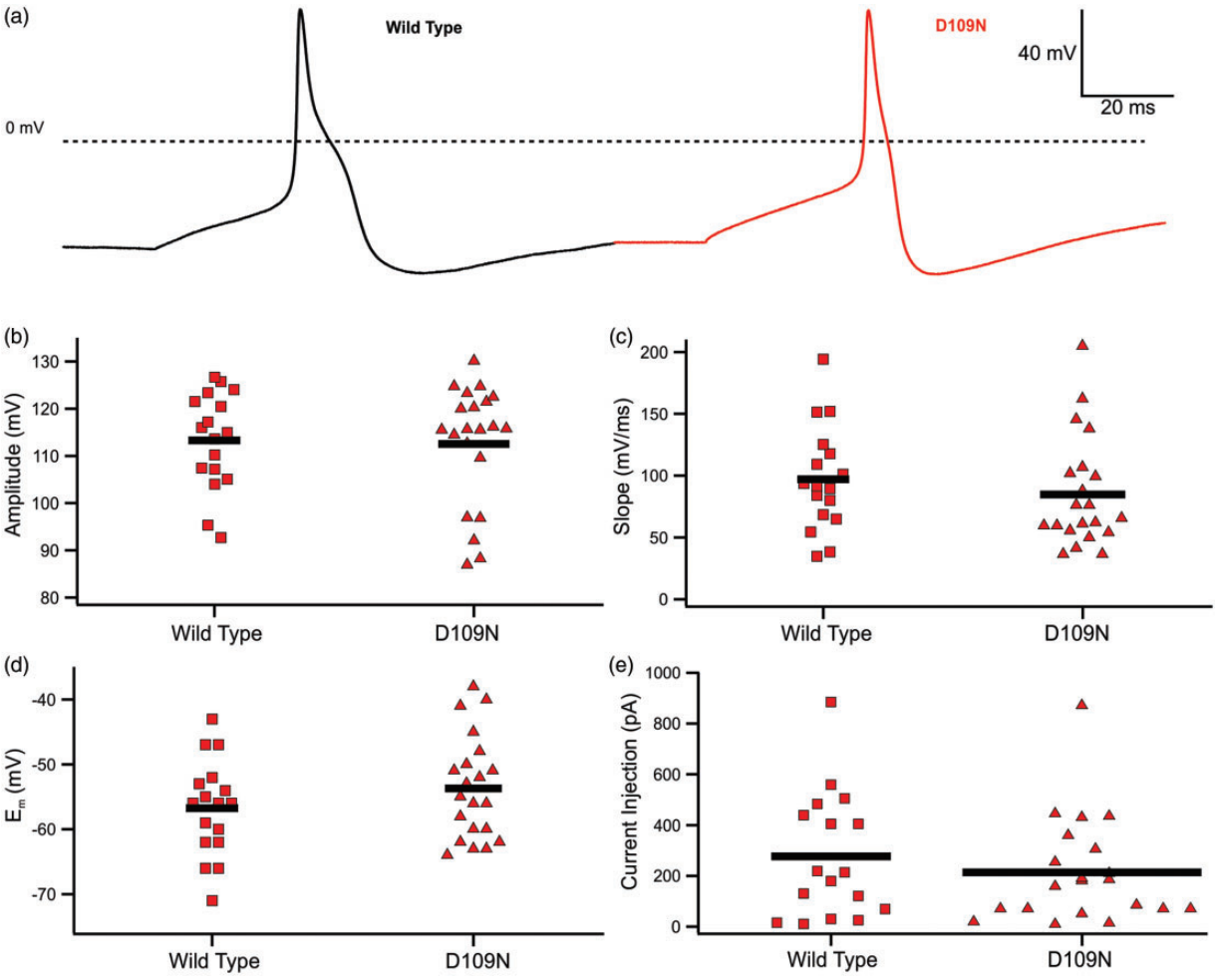

Figure 2. The β2 D109N variant does not alter passive membrane properties or action potential characteristics of DRG neurons. (a) Sample action potential waveforms representative of collected current-clamp recordings from either wild-type (n = 17) or D109N expressing DRG neurons (n = 21). (b) Comparison of total action potential amplitude for DRG neurons expressing either wild-type (113.28 ± 2.48 mV) or D109N variant (112.58 ± 2.85 mV, p = 0.85) β2-subunits. (c) Comparison of maximum slope during rising phase of action potential between DRG neurons expressing either wild-type (97.06 ± 10.21 mV/ms) or D109N variant (84.71 ± 10.22, p = 0.39). (d) Comparison of resting membrane potential of DRG neurons overexpressing either wild-type (−56.8 ± 1.8 mV) or D109N variant (−53.7 ± 1.7 mV, p = 0.12) subunit. (e) Comparison of current injection threshold for action potential spiking between DRG neurons expressing either wild-type (278.23 ± 60.40 pA) or D109N variant (213.57 ± 45.29 pA, p = 0.39) β2-subunit.

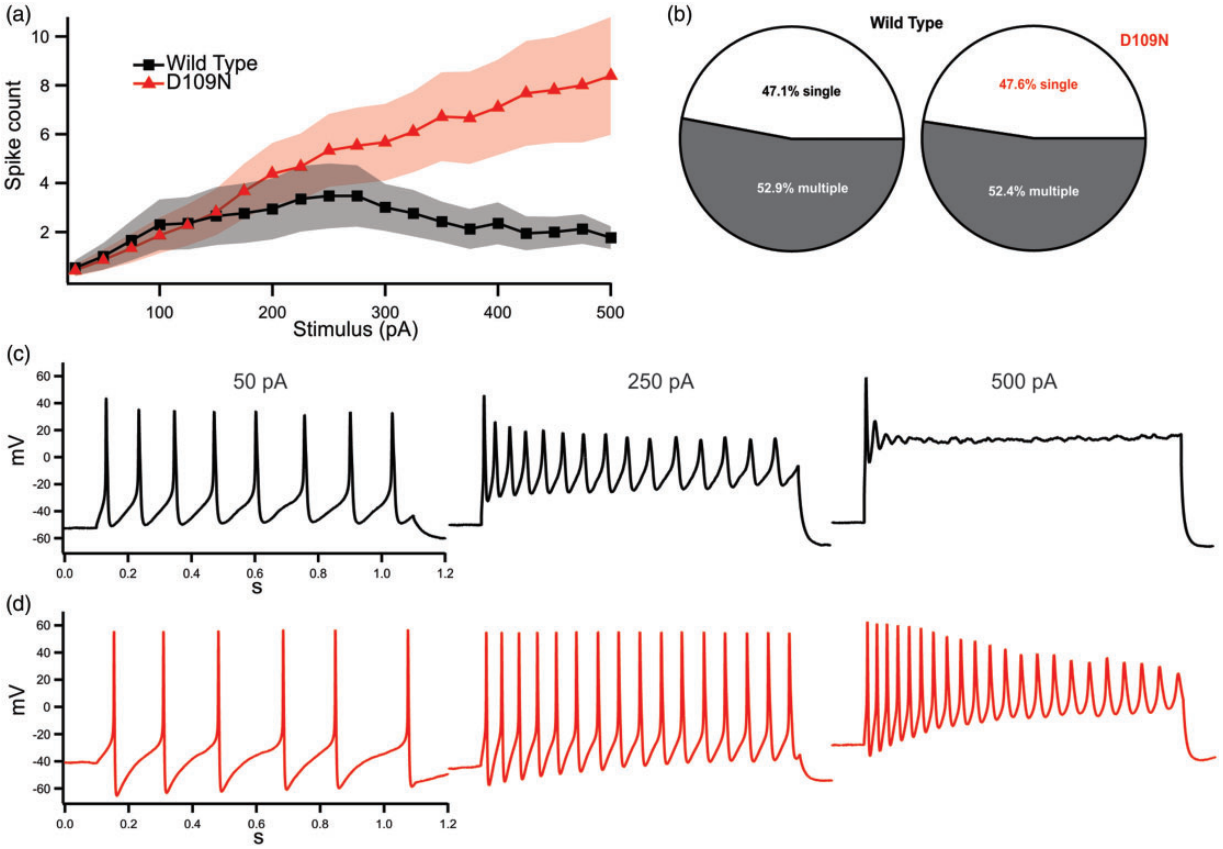

Figure 3. β2 D109N confers hyperexcitability to DRG neurons. (a) Comparison of repetitive action potential firing between DRG neurons expressing wild-type (n = 17) and D109N (n = 21) β2-subunits across a range of 500 ms current injections from 25 to 500 pA. Overexpression of β2-subunits with the D109N mutation permits continuous spiking of rat DRG neurons even in the presence of high-current stimuli, whereas DRG expressing wild-type β2-subunits adapt and cease firing. (b) The D109N mutation in the β2-subunit does not increase the proportion of cells that fire repetitively. Approximately 52% of neurons recorded in either condition fired multiple action potentials. (c and d) Sample traces at approximately threshold, 5× threshold, and 10× threshold for DRG cells expressing wild-type β2 (c, black) and mutant β2-subunits (d, red).

D109N mutation when compared against neurons expressing the wild-type β2-subunit (Figure 4(b)). Neurons expressing the β2 D109N variant allowed 82.9% of total charge transfer after 1 s of 20 Hz stimulation, which was not statistically different than the 78.3% allowed by neurons expressing the wild-type β2-subunit.

We also examined the change in current density as a function of the β2-subunit. As expected, there was no significant change in TTX-R current density between DRG neurons expressing the wild-type β2-subunit and those expressing the D109N variant; D109N-expressing DRG neurons exhibited a current density of 474.4 ± 149.2 pA/pF (n = 7), compared to 397.7 ± 85.9 pA/pF (n = 8) in wild-type-expressing DRG neurons (p = 0.65, data not shown). Interestingly, there was also no change in total current density between neurons expressing the wild-type (970.9 ± 50.9, n = 8) and D109N variant (975.5 ± 68.3, n = 12, p = 0.99) β2-subunit.

The β2 D109N variant depolarizes the voltage dependence of fast inactivation of total sodium current in DRG neurons

Classically, mutations in voltage-gated sodium channels found in peripheral neurons have been implicated in IEM, PEPD, and SFN. Mutations in $Na_v1.7$ that result in IEM tend to hyperpolarize the voltage dependence of channel activation,[9–12] whereas mutations that result in PEPD tend to depolarize the voltage dependence of sodium channel fast inactivation.[14,15,48] Mutations in $Na_v1.7$, $Na_v1.8$, and $Na_v1.9$ resulting in SFN often result in a spectrum of changes in channel gating.[16,22–24,49,50] Consequently, we examined whether the D109N variant in the β2-subunit altered properties of activation or fast inactivation of sodium channels in small DRG neurons. The β2 D109N variant results in no discernible change in the $V_{1/2}$ of activation (Figure 4(c)) for total sodium current in small DRG neurons (-20.14 ± 3.56 mV for neurons expressing the wild-type

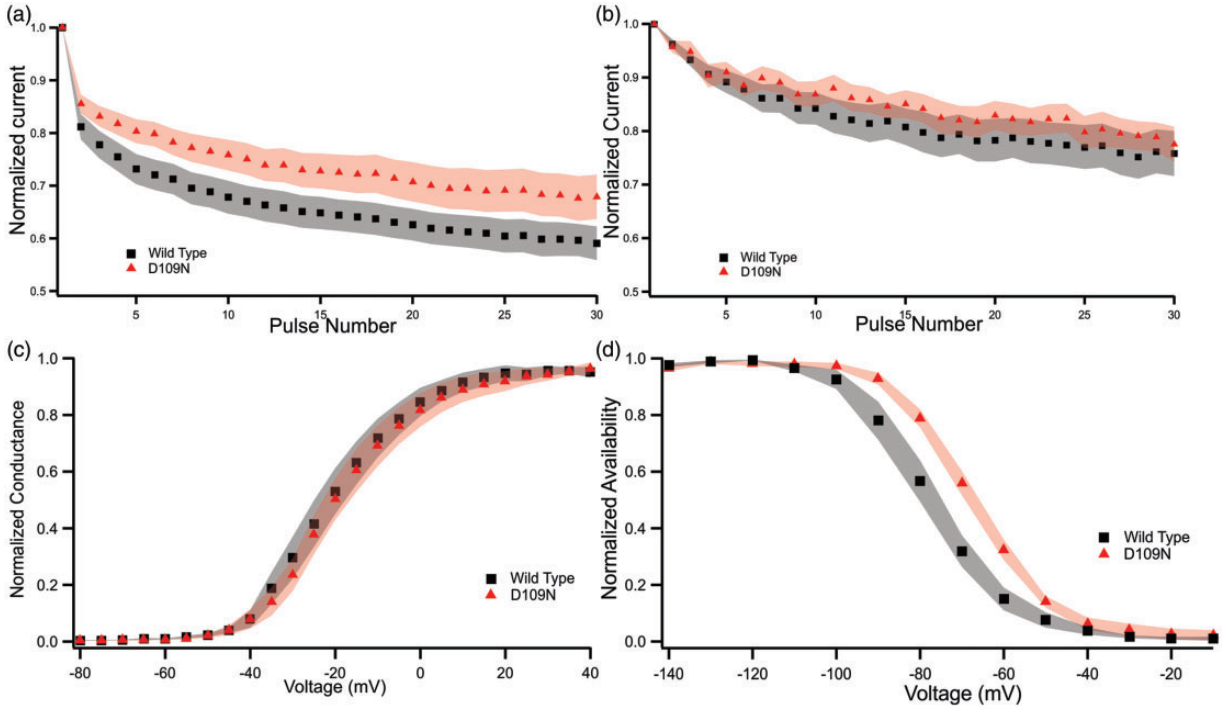

Figure 4. Voltage-clamp analysis of D109N variant. (a) Comparison of use-dependent inhibition of total sodium current after 20 Hz stimulation in DRG neurons expressing either wild-type (I/I_{max} at 1.5 s = 59.1%, n = 12) or D109N (I/I_{max} at 1.5 s = 67.9%, n = 14) β2-subunit. (b) Comparison of use-dependent inhibition of TTX-R sodium channels in DRG neurons expressing either wild-type (n = 8) or D109N variant (n = 9) showing no difference at 20 Hz stimulation. (c) Comparison of voltage dependence of activation in wild type (-20.1 ± 3.6 mV, n = 9) and D109N (-17.5 ± 4.3 mV, n = 9, p = 0.65). (d) Comparison of voltage dependence of fast inactivation in DRG neurons expressing either wild-type (-77.4 ± 2.7 mV, n = 8) or D109N variant (-67.8 ± 2.0 mV, n = 7).

β2-subunit vs. -17.53 ± 4.31 mV for neurons expressing the β2 D109N variant). However, the $V_{1/2}$ of fast inactivation (Figure 4(d)) was significantly more depolarized by 10 mV in small DRG neurons expressing the β2 D109N variant (-67.81 ± 1.97 mV) than the wild-type β2-subunit (-77.44 ± 2.71 mV, p = 0.015).

The β2 D109N variant modulates $Na_v1.7$ function, reducing use-dependent inhibition, and depolarizing the channel's voltage dependence of fast inactivation

Given that there was no change in TTX-R channel use dependence, the fast-inactivation curves were well fitted using a single Boltzmann function and the voltage dependence of inactivation was close to the expected value for $Na_v1.7$, and given that $Na_v1.7$ accounts for roughly 70% of TTX-S current in small DRG neurons,[51] we next examined whether the β2 D109N modulated gating properties of $Na_v1.7$. As HEK293 cells do not express appreciable levels of endogenous sodium currents (typically < 200 pA), stable cell lines expressing only $Na_v1.7$ were transfected with either the wild-type β2-subunit or the β2 D109N mutant. HEK293 cells expressing β2 D109N exhibited a rightward shift in the voltage dependence of fast inactivation when compared to cells expressing wild-type β2, similar to what was observed in DRG neurons (Figure 5(a)). The $V_{1/2}$ of fast inactivation for $Na_v1.7$ in the presence of β2 D109N was -75.95 mV, approximately 6.93 mV more depolarized than $Na_v1.7$ in the presence of wild-type β2 ($V_{1/2} = -82.87$, p = 0.043). Given also that a reduction in use-dependent inhibition of TTX-S channels was observed in DRG neurons, we investigated whether the β2 D109N mutant also directly affected the channel use-dependence properties of $Na_v1.7$ (Figure 5(b)). The presence of the β2 D109N-subunit resulted in reduced $Na_v1.7$ use-dependent inhibition after 1.5 s of 20 Hz stimulation (85% current remaining vs. 76%, statistically significant by two-way ANOVA with repeated measures).

Discussion

DPN is a chronic complication of DM that affects all aspects of patients' lives, with DPN being painful in only a subset of patients.[52] Painful variants of DPN are currently poorly managed by typical analgesics.[53] Consequently, there is a need for both better understanding of factors that predispose one to painful neuropathy and therapy targeted to the mechanism

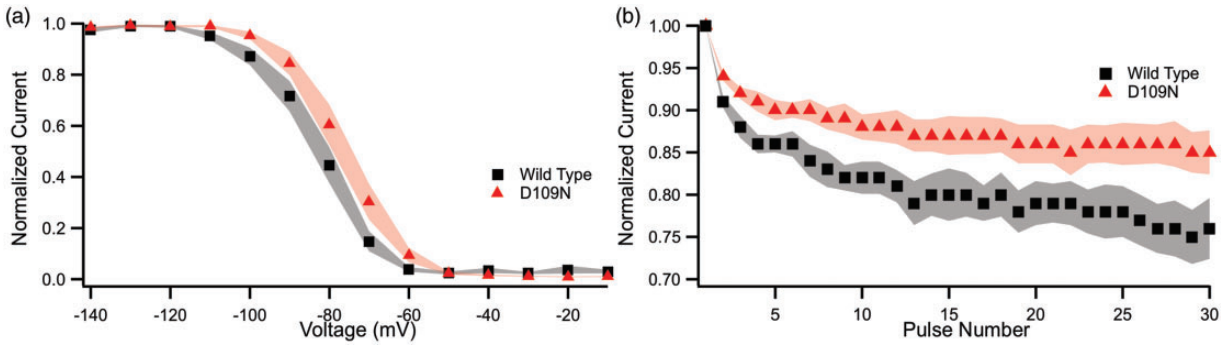

Figure 5. Voltage-clamp analysis of $Na_v1.7$ in the presence of the $\beta2$ D109N-subunit. (a) Comparison of voltage dependence of fast inactivation of $Na_v1.7$ in the presence of the D109N variant (-76.0 ± 2.2 mV, n = 8) and the wild-type $\beta2$ (-82.9 ± 2.3 mV, n = 9, p = 0.043). (b) The presence of the D109N variant (n = 6) results in a 9% reduction in use-dependent inhibition of $Na_v1.7$ compared to wild-type $\beta2$ (n = 6) after 1.5 s of 20 Hz stimulation.

underlying the painful DPN. Only recently have studies attempted to link painful DPN to specific predisposing mutations. Blesneac et al. discovered 12 rare (<1% prevalence) $Na_v1.7$ variants in a cohort of patients with painful diabetic neuropathy that were not seen in patients with painless DPN.[54] Six of these variants had been previously described in other neuropathies, such as SFN, with five resulting in gain-of-function changes in $Na_v1.7$. Blesneac et al. characterized two of the six previously uncharacterized $Na_v1.7$ variants found in painful diabetic neuropathy patients and illustrated gain-of-function changes in the channels. Here, we report the first β-subunit mutation to contribute to the development of neuropathic pain and DPN.

Previous studies have implicated the $\beta2$-subunit in neuropathic pain; expression of the $\beta2$-subunit is upregulated in neuropathic pain following spared nerve injury, and knockout of the $\beta2$-subunit attenuates mechanical allodynia induced by nerve injury.[55] This injury-induced upregulation of the $\beta2$-subunit directly increases sodium conductance in response to nerve injury.[56] $\beta2$-null mice are also known to show reduced responses to mechanically and inflammatory painful stimuli. Thus, it follows that, like upregulation, a gain-of-function mutation in the $\beta2$-subunit could also result in neuropathic pain.

Our results show that the D109N variant in the $\beta2$-subunit enhances hyperexcitability in DRG neurons via a mechanism that enhances repetitive firing but does not reduce rheobase (Figures 2 and 3). It is interesting to note that the RMP of DRG neurons expressing the D109N variant (-53.7 ± 1.7 mV) is not different from the RMP of DRG neurons expressing wild-type $\beta2$ (-56.8 ± 1.8 mV), and, similarly, current threshold for action potential firing was not altered. Previous work using dynamic-clamp analysis of $Na_v1.7$ has shown that an increase in $Na_v1.7$ conductance of 25% results in statistically significant reductions in current threshold.[51] The D109N mutation imparts approximately a 100% increase in total sodium channel conductance (as isolated $Na_v1.7$ channel conductance was not assayed in DRG neurons) at RMP. Considering the D109N variant's strong effect on $Na_v1.7$ and this increase in total sodium channel conductance, we would have anticipated to observe a reduction in rheobase. One explanation might be a possible effect of sodium channel β-subunits on other ion channels. In addition to modulating sodium channels, the β-subunits also interact with potassium channels, having been shown to coprecipitate with them and increase their current density.[57,58] Thus, the net interactions of the D109N with all of its ion channel partners precluded a reduction in rheobase.

However, neurons expressing β-subunits with this mutation continued to fire repetitively in response to large current injections, whereas neurons expressing the wild-type $\beta2$-subunit would adapt and attenuate their firing at larger current injections. We investigated the effect of variant D109N on channel use dependence as a conduit for enhancing repetitive firing and found that the $\beta2$ D109N variant resulted in reduced use dependence of firing in DRG neurons. This presumably allows repetitive firing by permitting a higher proportion of channels to continue to gate, rather than inactivate. Interestingly, this did not result in an increase in current density (Figure 4). However, this is not surprising given the fact that current density is a function of peak current during an activation pulse, and our primary hyperexcitability phenotype is reduced use-dependent inhibition. In addition, the expression system utilized involved overexpressing human $\beta2$-subunits in rat DRGs already expressing their normal β-subunits, potentially limiting how much current density could be increased.

We intended to next find the specific α-subunit by which the mutant $\beta2$-subunit acted to produce hyperexcitability. Sodium channel $\beta2$-subunits have been previously shown to regulate the TTX-S channels in DRG

neurons,[56] which is consistent with the results of this present study as we saw no change in the use dependence of TTX-R sodium channels. In addition to a reduction in use-dependent inhibition, presumably mediated via TTX-S Na_vs, in DRG neurons (which could include Na_v1.3, 1.6, and 1.7), we also elucidated a gain-of-function change in the voltage dependence of fast inactivation for total sodium current. This is consistent with previous studies that implicated a role for the β2-subunit in modulating inactivation but not activation of sodium channels in neurons; Chen et al. showed that knocking out the β2-subunit results in a hyperpolarized shift of 10.6 mV in the half-inactivation voltage to sodium current for hippocampal neurons, consistent with a loss-of-function attribute of the mutation.[59] Here, we report a gain-of-function mutation that results in a depolarizing shift in the voltage dependence of fast inactivation of the total sodium current within DRG neurons by approximately 9.64 mV. This biophysical finding is consistent with mutations that result in other pain syndromes, specifically PEPD.[15,48] As individual traces recorded were all well fit with a single Boltzmann and the overall $V_{1/2}$ of fast inactivation was similar to that of Na_v1.7,[60] which is responsible for the majority of the TTX-S current in small DRG neurons,[51] we then investigated if the mutant β2-subunit modulated Na_v1.7. The D109N mutation resulted in a 6.93 mV shift in the fast inactivation of Na_v1.7 (Figure 5(a)), approximately 72% of the total 9.64 mV shift seen in DRG neurons. This is concordant with the previous finding that Na_v1.7 is responsible for approximately 70% of TTX-S current in DRG neurons.[51] What this also implies, however, is that Na_v1.7 may not be the only Nav modulated by the D109N mutant β2-subunit and other TTX-S channels, such as Na_v1.6, may also play a role—although not as pronounced as Na_v1.7.

While the patient's painful phenotype is congruent with DRG hyperexcitability and gain-of-function changes in use-dependent inhibition and voltage dependence of fast inactivation of Na_v1.7, the question of the mechanism underpinning these changes remains unknown. Das et al. elucidated the crystal structure of the β2-subunit to 1.35 Å resolution and discovered that the cysteine at residue 55 of the β2-subunit forms a disulfide bond with the cysteine at residue 910 in the Domain II S5–S6 linker of Na_v1.2, a neuronal sodium channel found predominantly in the central nervous system.[43] As the D109N mutation shares a surface with the C55 residue on the β2-subunit, it is plausible that it interacts with the Domain II S5–S6 linker region to exert its gain-of-function effects on Na_v1.7 (and potentially other TTX-S channels). Indeed, mutations in the Domain II S5–S6 linker of TTX-S channels have been linked to different pain syndromes—both increased and decreased,[16,61] highlighting a role for this region in the development of neuropathic pain.[62] In addition, Das et al. suggest that the β2-subunit may position itself between either the voltage sensor domains (VSDs) of Domains I and II or between VSD I and VSD IV.[43] Given the importance of Domain IV in controlling fast inactivation in sodium channels,[63–67] it is possible that the D109N variant also exerts some effect on this locus. It has also recently been shown that human β-subunits directly modulate individual VSDs, providing compelling evidence for direct interactions with VSDs.[68] Of note, the inactivated structure of human Na_v1.7 in complex with the β1 and β2 structures was recently solved.[69] Although a source of vast and important information regarding Na_v1.7 structure, we avoid drawing conclusions on interactions between the α-subunit and the β-subunits from this structure because the β-subunits were resolved at a low resolution (4–5 Å) and showed quite flexible docking, making it difficult to draw conclusive information on their location. Further work is needed to evaluate whether other mutations in the β2-subunit (as well as other β-subunits) result in pain syndromes and, if so, through what mechanisms and which specific α-subunits. Here, we show that the D109N variant in the β2-subunit exerts an effect on fast inactivation and use-dependent inhibition in Na_v1.7, but there may be other mechanisms associated with other β-subunit mutations.

Acknowledgments

The authors would like to acknowledge Peng Zhao and Lawrence Macala for technical assistance. The authors would also like to thank Fadia Dib-Hajj for preparation of DNA constructs. This material is the result of work supported with resources and the use of facilities at the VA Medical Center West Haven. The contents do not represent the views of the U. S. Department of Veterans Affairs or the United States Government.

Propane Study Group: B de Greef (the Netherlands), JGJ Hoeijmakers (the Netherlands), M Sopacua (the Netherlands), HJM Smeets (the Netherlands), JM Vanoevelen (the Netherlands), I Eijkenboom (the Netherlands), P Lindsey (the Netherlands), R Almomani (the Netherlands), M Taiana (Italy), M Marchi (Italy), R Lombardi (Italy), D Cazzato (Italy), FM Boneschi (Italy), A Zauli (Italy), F Clarelli (Italy), S Santoro (Italy), I Lopez, A Quattrini (Italy), S Cestèle, O Chever, M Tavakoli, R Malik, D Kapetis, MN Xenakis (the Netherlands), M Mantegazza (France), F Battiato (Germany), A Strom (Germany), S Cestèle (France), O Chever (France), and R Malik (United Kingdom).

Declaration of Conflicting Interests

The author(s) declared no potential conflicts of interest with respect to the research, authorship, and/or publication of this article.

Funding

The author(s) disclosed receipt of the following financial support for the research, authorship, and/or publication of this article: This project was supported by grant 602273 from the European Union Seventh Framework Programme FP7/2007–2013 and by grants from the Rehabilitation Research Service, Department of Veterans Affairs. The Center for Neuroscience & Regeneration Research is a Collaboration of the Paralyzed Veterans of America with Yale University.

ORCID iD

Matthew Alsaloum https://orcid.org/0000-0002-9832-0138

References

1. Carracher AM, Marathe PH and Close KL. International diabetes federation 2017. *J Diabetes* 2018; 10: 353–356.
2. Young MJ, Boulton AJ, MacLeod AF, Williams DR and Sonksen PH. A multicentre study of the prevalence of diabetic peripheral neuropathy in the United Kingdom hospital clinic population. *Diabetologia* 1993; 36: 150–154.
3. Dyck PJ, Kratz KM, Karnes JL, Litchy WJ, Klein R, Pach JM, Wilson DM, O'Brien PC, Melton LJ III and Service FJ. The prevalence by staged severity of various types of diabetic neuropathy, retinopathy, and nephropathy in a population-based cohort: the Rochester Diabetic Neuropathy Study. *Neurology* 1993; 43: 817–824.
4. Shulman GI. Ectopic fat in insulin resistance, dyslipidemia, and cardiometabolic disease. *N Engl J Med* 2014; 371: 1131–1141.
5. Yan SD, Schmidt AM, Anderson GM, Zhang J, Brett J, Zou YS, Pinsky D and Stern D. Enhanced cellular oxidant stress by the interaction of advanced glycation end products with their receptors/binding proteins. *J Biol Chem* 1994; 269: 9889–9897.
6. Xia P, Kramer RM and King GL. Identification of the mechanism for the inhibition of Na+,K(+)-adenosine triphosphatase by hyperglycemia involving activation of protein kinase C and cytosolic phospholipase A2. *J Clin Invest* 1995; 96: 733–740.
7. Hoeijmakers JG, Merkies IS, Gerrits MM, Waxman SG and Faber CG. Genetic aspects of sodium channelopathy in small fiber neuropathy. *Clin Genet* 2012; 82: 351–358.
8. Yang Y, Wang Y, Li S, Xu Z, Li H, Ma L, Fan J, Bu D, Liu B, Fan Z, Wu G, Jin J, Ding B, Zhu X and Shen Y. Mutations in SCN9A, encoding a sodium channel alpha subunit, in patients with primary erythermalgia. *J Med Genet* 2004; 41: 171–174. 2004/02/27.
9. Cummins TR, Dib HS and Waxman SG. Electrophysiological properties of mutant Nav1.7 sodium channels in a painful inherited neuropathy. *J Neurosci* 2004; 24: 8232–8236.
10. Dib-Hajj SD, Rush AM, Cummins TR, Hisama FM, Novella S, Tyrrell L, Marshall L and Waxman SG. Gain-of-function mutation in Nav1.7 in familial erythromelalgia induces bursting of sensory neurons. *Brain* 2005; 128: 1847–1854.
11. Han C, Rush AM, Dib-Hajj SD, Li S, Xu Z, Wang Y, Tyrrell L, Wang X, Yang Y and Waxman SG. Sporadic onset of erythermalgia: a gain-of-function mutation in Nav1.7. *Ann Neurol* 2006; 59: 553–558.
12. Lampert A, Dib-Hajj SD, Tyrrell L and Waxman SG. Size matters: erythromelalgia mutation S241T in Nav1.7 alters channel gating. *J Biol Chem* 2006; 281: 36029–36035.
13. Choi JS, Boralevi F, Brissaud O, Sanchez-Martin J, Te Morsche RH, Dib-Hajj SD, Drenth JP and Waxman SG. Paroxysmal extreme pain disorder: a molecular lesion of peripheral neurons. *Nat Rev Neurol* 2011; 7: 51–55.
14. Fertleman CR, Baker MD, Parker KA, Moffatt S, Elmslie FV, Abrahamsen B, Ostman J, Klugbauer N, Wood JN, Gardiner RM and Rees M. SCN9A mutations in paroxysmal extreme pain disorder: allelic variants underlie distinct channel defects and phenotypes. *Neuron* 2006; 52: 767–774.
15. Jarecki BW, Sheets PL, Jackson JO and Cummins TR. Paroxysmal extreme pain disorder mutations within the D3/S4-S5 linker of Nav1.7 cause moderate destabilization of fast inactivation. *J Physiol* 2008; 586: 4137–4153.
16. Faber CG, Hoeijmakers JG, Ahn HS, Cheng X, Han C, Choi JS, Estacion M, Lauria G, Vanhoutte EK, Gerrits MM, Dib-Hajj S, Drenth JP, Waxman SG and Merkies IS. Gain of function Nanu1.7 mutations in idiopathic small fiber neuropathy. *Ann Neurol* 2012; 71: 26–39.
17. Ahmad S, Dahllund L, Eriksson AB, Hellgren D, Karlsson U, Lund PE, Meijer IA, Meury L, Mills T, Moody A, Morinville A, Morten J, O'Donnell D, Raynoschek C, Salter H, Rouleau GA and Krupp JJ. A stop codon mutation in SCN9A causes lack of pain sensation. *Hum Mol Genet* 2007; 16: 2114–2121.
18. Cox JJ, Reimann F, Nicholas AK, Thornton G, Roberts E, Springell K, Karbani G, Jafri H, Mannan J, Raashid Y, Al-Gazali L, Hamamy H, Valente EM, Gorman S, Williams R, McHale DP, Wood JN, Gribble FM and Woods CG. An SCN9A channelopathy causes congenital inability to experience pain. *Nature* 2006; 444: 894–898.
19. Goldberg YP, MacFarlane J, MacDonald ML, Thompson J, Dube MP, Mattice M, Fraser R, Young C, Hossain S, Pape T, Payne B, Radomski C, Donaldson G, Ives E, Cox J, Younghusband HB, Green R, Duff A, Boltshauser E, Grinspan GA, Dimon JH, Sibley BG, Andria G, Toscano E, Kerdraon J, Bowsher D, Pimstone SN, Samuels ME, Sherrington R and Hayden MR. Loss-of-function mutations in the Nav1.7 gene underlie congenital indifference to pain in multiple human populations. *Clin Genet* 2007; 71: 311–319.
20. Tanaka BS, Zhao P, Dib-Hajj FB, Morisset V, Tate S, Waxman SG and Dib-Hajj SD. A gain-of-function mutation in Nav1.6 in a case of trigeminal neuralgia. *Mol Med* 2016; 22: 338–348.
21. Chen L, Huang J, Zhao P, Persson AK, Dib-Hajj FB, Cheng X, Tan A, Waxman SG and Dib-Hajj SD. Conditional knockout of NaV1.6 in adult mice ameliorates neuropathic pain. *Sci Rep* 2018; 8: 3845.
22. Faber CG, Lauria G, Merkies IS, Cheng X, Han C, Ahn HS, Persson AK, Hoeijmakers JG, Gerrits MM, Pierro T, Lombardi R, Kapetis D, Dib-Hajj SD and Waxman SG.

Gain-of-function Nav1.8 mutations in painful neuropathy. *Proc Natl Acad Sci USA* 2012; 109: 19444–19449.
23. Huang J, Han C, Estacion M, Vasylyev D, Hoeijmakers JG, Gerrits MM, Tyrrell L, Lauria G, Faber CG, Dib-Hajj SD, Merkies IS, Waxman SG and Group PS. Gain-of-function mutations in sodium channel Na(v)1.9 in painful neuropathy. *Brain* 2014; 137: 1627–1642.
24. Huang J, Yang Y, Zhao P, Gerrits MM, Hoeijmakers JG, Bekelaar K, Merkies IS, Faber CG, Dib-Hajj SD and Waxman SG. Small-fiber neuropathy Nav1.8 mutation shifts activation to hyperpolarized potentials and increases excitability of dorsal root ganglion neurons. *J Neurosci* 2013; 33: 14087–14097.
25. Han C, Yang Y, Te Morsche RH, Drenth JP, Politei JM, Waxman SG and Dib-Hajj SD. Familial gain-of-function Nav1.9 mutation in a painful channelopathy. *J Neurol Neurosurg Psychiatry* 2017; 88: 233–240.
26. Zhang XY, Wen J, Yang W, Wang C, Gao L, Zheng LH, Wang T, Ran K, Li Y, Li X, Xu M, Luo J, Feng S, Ma X, Ma H, Chai Z, Zhou Z, Yao J, Zhang X and Liu JY. Gain-of-function mutations in SCN11A cause familial episodic pain. *Am J Hum Genet* 2013; 93: 957–966.
27. Han C, Vasylyev D, Macala LJ, Gerrits MM, Hoeijmakers JG, Bekelaar KJ, Dib-Hajj SD, Faber CG, Merkies IS and Waxman SG. The G1662S NaV1.8 mutation in small fibre neuropathy: impaired inactivation underlying DRG neuron hyperexcitability. *J Neurol Neurosurg Psychiatry* 2014; 85: 499–505.
28. Han C, Yang Y, de Greef BT, Hoeijmakers JG, Gerrits MM, Verhamme C, Qu J, Lauria G, Merkies IS, Faber CG, Dib-Hajj SD and Waxman SG. The domain II S4–S5 linker in Nav1.9: a missense mutation enhances activation, impairs fast inactivation, and produces human painful neuropathy. *Neuromolecular Med* 2015; 17: 158–169.
29. Bouza AA and Isom LL. Voltage-gated sodium channel beta subunits and their related diseases. *Handb Exp Pharmacol* 2018; 246: 423–450.
30. Chahine M and O'Leary ME. Regulatory role of voltage-gated Na channel beta subunits in sensory neurons. *Front Pharmacol* 2011; 2: 70–11.
31. O'Malley HA and Isom LL. Sodium channel beta subunits: emerging targets in channelopathies. *Annu Rev Physiol* 2015; 77: 481–504.
32. Xiao ZC, Ragsdale DS, Malhotra JD, Mattei LN, Braun PE, Schachner M and Isom LL. Tenascin-R is a functional modulator of sodium channel beta subunits. *J Biol Chem* 1999; 274: 26511–26517.
33. Shimizu H, Tosaki A, Ohsawa N, Ishizuka-Katsura Y, Shoji S, Miyazaki H, Oyama F, Terada T, Shirouzu M, Sekine SI, Nukina N and Yokoyama S. Parallel homodimer structures of the extracellular domains of the voltage-gated sodium channel beta4 subunit explain its role in cell-cell adhesion. *J Biol Chem* 2017; 292: 13428–13440.
34. Brackenbury WJ, Calhoun JD, Chen C, Miyazaki H, Nukina N, Oyama F, Ranscht B and Isom LL. Functional reciprocity between Na+ channel Nav1.6 and beta1 subunits in the coordinated regulation of excitability and neurite outgrowth. *Proc Natl Acad Sci USA* 2010; 107: 2283–2288.
35. Cummins TR, Aglieco F, Renganathan M, Herzog RI, Dib-Hajj SD and Waxman SG. Nav1.3 sodium channels: rapid repriming and slow closed-state inactivation display quantitative differences after expression in a mammalian cell line and in spinal sensory neurons. *J Neurosci* 2001; 21: 5952–5961.
36. Maxwell C. Sensitivity and accuracy of the Visual Analogue Scale: a psycho-physical classroom experiment. *Br J Clin Pharmacol* 1978; 6: 15–24.
37. Galer BS and Jensen MP. Development and preliminary validation of a pain measure specific to neuropathic pain: the Neuropathic Pain Scale. *Neurology* 1997; 48: 332–338.
38. Bonhof GJ, Strom A, Puttgen S, Ringel B, Bruggemann J, Bodis K, Mussig K, Szendroedi J, Roden M and Ziegler D. Patterns of cutaneous nerve fibre loss and regeneration in type 2 diabetes with painful and painless polyneuropathy. *Diabetologia* 2017; 60: 2495–2503.
39. Tesfaye S, Boulton AJ, Dyck PJ, Freeman R, Horowitz M, Kempler P, Lauria G, Malik RA, Spallone V, Vinik A, Bernardi L, Valensi P and Toronto Diabetic Neuropathy Expert Group. Diabetic neuropathies: update on definitions, diagnostic criteria, estimation of severity, and treatments. *Diabetes Care* 2010; 33: 2285–2293.
40. Treede RD, Jensen TS, Campbell JN, Cruccu G, Dostrovsky JO, Griffin JW, Hansson P, Hughes R, Nurmikko T and Serra J. Neuropathic pain: redefinition and a grading system for clinical and research purposes. *Neurology* 2008; 70: 1630–1635.
41. O'Roak BJ, Vives L, Fu W, Egertson JD, Stanaway IB, Phelps IG, Carvill G, Kumar A, Lee C, Ankenman K, Munson J, Hiatt JB, Turner EH, Levy R, O'Day DR, Krumm N, Coe BP, Martin BK, Borenstein E, Nickerson DA, Mefford HC, Doherty D, Akey JM, Bernier R, Eichler EE and Shendure J. Multiplex targeted sequencing identifies recurrently mutated genes in autism spectrum disorders. *Science* 2012; 338: 1619–1622.
42. Wallis Y, Payne S, McAnulty C, Bodmer D, Sistermans E, Robertson K, Moore D, Abbs S, Deans Z and Devereau A. Practice guidelines for the evaluation of pathogenicity and the reporting of sequence variants in clinical molecular genetics, 2013,https://pdfs.semanticscholar.org/330d/d56c5b8e912650410e9c0c87404a6c4b09ec.pdf.
43. Das S, Gilchrist J, Bosmans F and Van Petegem F. Binary architecture of the Nav1.2-beta2 signaling complex. *Elife* 2016; 5: e10960.
44. Dib-Hajj SD, Choi JS, Macala LJ, Tyrrell L, Black JA, Cummins TR and Waxman SG. Transfection of rat or mouse neurons by biolistics or electroporation. *Nat Protoc* 2009; 4: 1118–1126.
45. Karczewski KJ, Francioli LC, Tiao G, Cummings BB, Alföldi J, Wang Q, Collins RL, Laricchia KM, Ganna A, Birnbaum DP, Gauthier LD, Brand H, Solomonson M, Watts NA, Rhodes D, Singer-Berk M, Seaby EG, Kosmicki JA, Walters RK, Tashman K, Farjoun Y, Banks E, Poterba T, Wang A, Seed C, Whiffin N, Chong JX, Samocha KE, Pierce-Hoffman E, Zappala Z, O'Donnell-Luria AH, Vallabh Minikel E, Weisburd B, Lek M, Ware JS, Vittal C, Armean IM, Bergelson L, Cibulskis K, Connolly KM, Covarrubias M, Donnelly S, Ferriera S, Gabriel S, Gentry J, Gupta N, Jeandet T,

Kaplan D, Llanwarne C, Munshi R, Novod S, Petrillo N, Roazen D, Ruano-Rubio V, Saltzman A, Schleicher M, Soto J, Tibbetts K, Tolonen C, Wade G, Talkowski ME, Neale BM, Daly MJ and MacArthur DG. Variation across 141,456 human exomes and genomes reveals the spectrum of loss-of-function intolerance across human protein-coding genes. *BioRxiv*. Epub ahead of print 28 January 2019. DOI: 10.1101/531210.

46. Naundorf B, Wolf F and Volgushev M. Unique features of action potential initiation in cortical neurons. *Nature* 2006; 440: 1060–1063.
47. McLean MJ and Macdonald RL. Carbamazepine and 10,11-epoxycarbamazepine produce use- and voltage-dependent limitation of rapidly firing action potentials of mouse central neurons in cell culture. *J Pharmacol Exp Ther* 1986; 238: 727–738.
48. Dib-Hajj SD, Estacion M, Jarecki BW, Tyrrell L, Fischer TZ, Lawden M, Cummins TR and Waxman SG. Paroxysmal extreme pain disorder M1627K mutation in human Nav1.7 renders DRG neurons hyperexcitable. *Mol Pain* 2008; 4: 37.
49. Estacion M, Han C, Choi JS, Hoeijmakers JG, Lauria G, Drenth JP, Gerrits MM, Dib-Hajj SD, Faber CG, Merkies IS and Waxman SG. Intra- and interfamily phenotypic diversity in pain syndromes associated with a gain-of-function variant of NaV1.7. *Mol Pain* 2011; 7: 92.
50. Han C, Hoeijmakers JG, Ahn HS, Zhao P, Shah P, Lauria G, Gerrits MM, Te Morsche RH, Dib-Hajj SD, Drenth JP, Faber CG, Merkies IS and Waxman SG. Nav1.7-related small fiber neuropathy: impaired slow-inactivation and DRG neuron hyperexcitability. *Neurology* 2012; 78: 1635–1643.
51. Vasylyev DV, Han C, Zhao P, Dib-Hajj S and Waxman SG. Dynamic-clamp analysis of wild-type human Nav1.7 and erythromelalgia mutant channel L858H. *J Neurophysiol* 2014; 111: 1429–1443.
52. Brod M, Pohlman B, Blum SI, Ramasamy A and Carson R. Burden of illness of diabetic peripheral neuropathic pain: a qualitative study. *Patient* 2015; 8: 339–348.
53. Finnerup NB, Attal N, Haroutounian S, McNicol E, Baron R, Dworkin RH, Gilron I, Haanpaa M, Hansson P, Jensen TS, Kamerman PR, Lund K, Moore A, Raja SN, Rice AS, Rowbotham M, Sena E, Siddall P, Smith BH and Wallace M. Pharmacotherapy for neuropathic pain in adults: a systematic review and meta-analysis. *Lancet Neurol* 2015; 14: 162–173.
54. Blesneac I, Themistocleous AC, Fratter C, Conrad LJ, Ramirez JD, Cox JJ, Tesfaye S, Shillo PR, Rice ASC, Tucker SJ and Bennett D. Rare NaV1.7 variants associated with painful diabetic peripheral neuropathy. *Pain* 2018; 159: 469–480.
55. Pertin M, Ji RR, Berta T, Powell AJ, Karchewski L, Tate SN, Isom LL, Woolf CJ, Gilliard N, Spahn DR and Decosterd I. Upregulation of the voltage-gated sodium channel beta2 subunit in neuropathic pain models: characterization of expression in injured and non-injured primary sensory neurons. *J Neurosci* 2005; 25: 10970–10980.
56. Lopez-Santiago LF, Pertin M, Morisod X, Chen C, Hong S, Wiley J, Decosterd I and Isom LL. Sodium channel beta2 subunits regulate tetrodotoxin-sensitive sodium channels in small dorsal root ganglion neurons and modulate the response to pain. *J Neurosci* 2006; 26: 7984–7994.
57. Nguyen HM, Miyazaki H, Hoshi N, Smith BJ, Nukina N, Goldin AL and Chandy KG. Modulation of voltage-gated K+ channels by the sodium channel beta1 subunit. *Proc Natl Acad Sci USA* 2012; 109: 18577–18582.
58. Marionneau C, Carrasquillo Y, Norris AJ, Townsend RR, Isom LL, Link AJ and Nerbonne JM. The sodium channel accessory subunit Navbeta1 regulates neuronal excitability through modulation of repolarizing voltage-gated K(+) channels. *J Neurosci* 2012; 32: 5716–5727.
59. Chen C, Bharucha V, Chen Y, Westenbroek RE, Brown A, Malhotra JD, Jones D, Avery C, Gillespie PJ, Kazen-Gillespie KA, Kazarinova-Noyes K, Shrager P, Saunders TL, Macdonald RL, Ransom BR, Scheuer T, Catterall WA and Isom LL. Reduced sodium channel density, altered voltage dependence of inactivation, and increased susceptibility to seizures in mice lacking sodium channel beta 2-subunits. *Proc Natl Acad Sci USA* 2002; 99: 17072–17077.
60. Vijayaragavan K, O'Leary ME and Chahine M. Gating properties of Na(v)1.7 and Na(v)1.8 peripheral nerve sodium channels. *J Neurosci* 2001; 21: 7909–7918.
61. Cox JJ, Sheynin J, Shorer Z, Reimann F, Nicholas AK, Zubovic L, Baralle M, Wraige E, Manor E, Levy J, Woods CG and Parvari R. Congenital insensitivity to pain: novel SCN9A missense and in-frame deletion mutations. *Hum Mutat* 2010; 31: E1670–E1686.
62. Huang W, Liu M, Yan SF and Yan N. Structure-based assessment of disease-related mutations in human voltage-gated sodium channels. *Protein Cell* 2017; 8: 401–438.
63. McPhee JC, Ragsdale DS, Scheuer T and Catterall WA. A critical role for the S4-S5 intracellular loop in domain IV of the sodium channel alpha-subunit in fast inactivation. *J Biol Chem* 1998; 273: 1121–1129.
64. McPhee JC, Ragsdale DS, Scheuer T and Catterall WA. A critical role for transmembrane segment IVS6 of the sodium channel alpha subunit in fast inactivation. *J Biol Chem* 1995; 270: 12025–12034.
65. McPhee JC, Ragsdale DS, Scheuer T and Catterall WA. A mutation in segment IVS6 disrupts fast inactivation of sodium channels. *Proc Natl Acad Sci USA* 1994; 91: 12346–12350.
66. Luo S, Sampedro Castaneda M, Matthews E, Sud R, Hanna MG, Sun J, Song J, Lu J, Qiao K, Zhao C and Mannikko R. Hypokalaemic periodic paralysis and myotonia in a patient with homozygous mutation p.R1451L in NaV1.4. *Sci Rep* 2018; 8: 9714.
67. Capes DL, Goldschen-Ohm MP, Arcisio-Miranda M, Bezanilla F and Chanda B. Domain IV voltage-sensor movement is both sufficient and rate limiting for fast inactivation in sodium channels. *J Gen Physiol* 2013; 142: 101–112.
68. Zhu W, Voelker TL, Varga Z, Schubert AR, Nerbonne JM and Silva JR. Mechanisms of noncovalent beta subunit regulation of NaV channel gating. *J Gen Physiol*. Epub ahead of print 20 July 2017. DOI: 10.1085/jgp.201711802.
69. Shen H, Liu D, Wu K, Lei J and Yan N. Structures of human Nav1.7 channel in complex with auxiliary subunits and animal toxins. *Science* 2019; 363: 1303–1308.